

Multi-Loop PID Controller Design for PVA Degradation in a Tubular UV/H₂O₂ Photoreactor

Zahra Parsa¹, Ramdhane Dhib², Mehrab Mehrvar³

Department of Chemical Engineering, Toronto Metropolitan University, 350 Victoria Street, Toronto, Ontario, Canada, M5B 2K3

¹e-mail:zahra.parsa@tororntomu.ca, ²e-mail:rdhib@tororntomu.ca,

³e-mail:mmehrvar@tororntomu.ca

Abstract: Despite significant progress in advanced process control strategies and their performances, proportional-integral-derivative feedback (PID-FB) control remains one of the prevailing approaches in real applications. The popularity of PID controllers is attributed to their simplicity, straightforward implementation, and applicability, especially for single-input, single-output (SISO) systems. However, most industrial processes are multi-input multi-output (MIMO), with pronounced process interactions, necessitating multi-loop control. Identifying these interactions, choosing the optimal pairs of manipulated variables (MVs) and controlled variables (CVs) for MIMO control, and implementing strategies to mitigate system interactions are critical and challenging. This study investigates a multiple PID-FB loop control strategy for a UV/H₂O₂ photoreactor utilized to degrade polyvinyl alcohol (PVA) in an aqueous solution. The control objective is to regulate the effluent total organic carbon (TOC) and residual H₂O₂ concentrations (mg/L) while mitigating the impact of the inlet PVA concentration (mg/L) as a disturbance on CVs. The relative gain array (RGA) analysis is used to identify the interaction of control processes and determine the best MV/CV sets. Before controller design, the interaction between control loops is mitigated by designing the feedforward (FF) decouplers. Subsequently, PID controllers are tuned for each decoupled loop. The response of the decoupled system to setpoint trajectory and disturbance rejection affirms its excellent control performance. Additionally, the realizability of the designed decouplers is assessed. All simulations are conducted in MATLAB Simulink.

Keywords: process control; PID controller; MIMO system; decoupling; wastewater treatment; AOP; UV/H₂O₂; PID-FB multi-loop control; PVA; water soluble polymer

1. INTRODUCTION

Water-soluble polymers play a significant role in various industries, serving as raw materials in producing and processing diverse products. Polyvinyl alcohol (PVA) stands out as the most widely used synthetic water-soluble polymer, notably in the textile industry. However, the extensive use of this polymer contributes to the generation of substantial quantities of polymer-contained wastewater worldwide, posing severe risks to the environment and human health if released untreated (Hamad et al., 2018). Biological treatment is the conventional choice for addressing organic water pollutants unless the targeted compound proves non-biodegradable. Given the non-biodegradable nature of PVA, alternative methods such as advanced oxidation processes (AOPs) have become essential (Parsa et al., 2022, 2023). The UV/H₂O₂ process has shown promise as an effective method for PVA removal, demonstrating efficient degradation in aqueous environments (Hamad, 2015; Lin et al., 2021). Yet, a critical concern revolves around maintaining safe residual H₂O₂ levels in the discharged effluent, keeping it below a threshold (≈ 5 mg/L) to ensure harmlessness to living organisms upon release into receiving water bodies. Simultaneously, it is essential to attain efficient PVA

degradation. Addressing these concerns concurrently necessitates optimization studies to minimize residual H₂O₂ while maximizing PVA removal (Hamad, 2015). As PVA degrades, it produces oligomers and monomers, and as degradation continues, mineralization occurs, resulting in the generation of CO₂ and water. The degradation mechanism alters the total organic carbon (TOC) content in the process effluent. TOC is a surrogate parameter commonly used in wastewater treatment plants to monitor influent and effluent quality. Thus, ensuring efficient TOC removal is a crucial goal in PVA degradation studies, representing the efficiency of the polymer degradation. Despite the optimization studies, actual processes often face deviations from their optimal operating conditions due to both measurable and unmeasurable disturbances. These deviations may lead to undesired increases in residual H₂O₂ and TOC content within the effluent. Addressing these challenges involves designing a control system capable of regulating the process to maintain the desired trajectory for both process outputs. This system would detect deviations from the setpoints and adjust the process by manipulating its inputs, effectively managing and mitigating undesirable outcomes. Multi-input multi-output (MIMO) systems pertain to systems wherein multiple controlled variables (CVs) necessitate control through the manipulation of multiple manipulated variables (MVs). This configuration

is prevalent in real industrial plants, often mandating the simultaneous control of multiple CVs. Despite the extensive research on advanced control strategies such as internal model control (IMC), model predictive control (MPC), or artificial intelligence (AI)-based controls, the predominant control strategy utilized in practical applications remains the implementation of a multi-loop proportional-integral-derivative (PID) control (Parsa et al., 2024). This approach comprises multiple feedback (FB) loops, each incorporating a PID controller that controls a specific CV. In MIMO systems, a crucial consideration is the inherent interaction or coupling among various control loops. Manipulating one MV to regulate a desired CV may undesirably impact other CVs concurrently. In the process control domain, systems exhibiting such interdependence are classified as systems with interactive loops (Garrido et al., 2016). Tuning controllers for systems characterized by significant interactions poses considerable challenges, and even the closed-loop system may exhibit instability (Astrom et al., 2001). Addressing control challenges in interactive systems is achievable by involving the initial decoupling of control loops followed by the subsequent design of controllers for each decoupled loop.

This study aims to analyze the MIMO process of PVA degradation in UV/H₂O₂ photoreactors. It involves assessing system interaction, decoupling the system, and designing PID-FB controllers for the decoupled loops to achieve effective performance in setpoint tracking and disturbance rejection.

2. EXPERIMENTAL SETUP AND PROCEDURE

The experimental configuration, depicted in Figure 1, comprises two 30 cm-long, 460 mL-volume photoreactors arranged in series. The setup includes three tanks for storing H₂O₂, PVA-contained wastewater, and collecting the treated effluent. Two peristaltic pumps are employed to deliver H₂O₂ and wastewater separately to the inlet of the photoreactors. The focus of this study is on degrading PVA-contained wastewater. Upon exposure to UV light within the photoreactor, H₂O₂ undergoes decomposition, generating reactive hydroxyl radicals. These radicals non-selectively target PVA molecules, breaking them into shorter molecules, carboxylic acids, CO₂ and water.

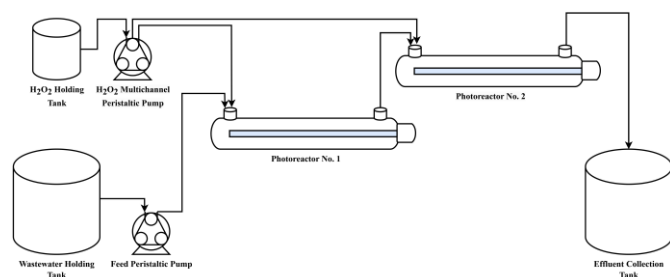


Figure 1. Schematic diagram of the lab-scale continuous UV/H₂O₂ system.

In a previous study (Hamad et al., 2021), the dynamic model for the studied process was formulated based on experimental data. The process operated continuously under specific operating conditions, including 1000 mg/L inlet PVA concentration, 585 mg/L inlet H₂O₂ concentration, and 100

mL/min PVA-contained wastewater flowrate, until reaching a steady state. Subsequently, 50% step changes were applied to each operating condition individually. Samples were collected every 30 seconds at the effluent for TOC and H₂O₂ concentration analysis until the next steady state was reached. The experimental data obtained from these runs were utilized to develop the process dynamic model, which will be elaborated in the following section.

3. PROCESS DYNAMIC MODEL

The vector-matrix notation of the relation between process variables in the Laplace domain for a continuous system is as follows:

$$\underline{y}(s) = \underline{G}_P(s) \cdot \underline{u}(s) + \underline{G}_d(s) \cdot \underline{d}(s) \quad (1)$$

Where, $\underline{y}(s)$ is the vector of outputs, $\underline{G}_P(s)$ is transfer matrix for the process, $\underline{u}(s)$ is the vector of process inputs, $\underline{G}_d(s)$ is transfer matrix of disturbances, and $\underline{d}(s)$ is the vector of disturbances. Equation (1) can be expanded into (2) as outlined below:

$$\begin{bmatrix} y_1 \\ y_2 \end{bmatrix} = \begin{bmatrix} G_{11} & G_{12} \\ G_{21} & G_{22} \end{bmatrix} \begin{bmatrix} u_1 \\ u_2 \end{bmatrix} + \begin{bmatrix} G_{13} \\ G_{23} \end{bmatrix} d \quad (2)$$

In this study, y_1 and y_2 are effluent TOC and residual H₂O₂ concentrations (mg/L), respectively. u_1 and u_2 are PVA feed flow rate (mL/min) and inlet H₂O₂ concentration (mg/L), respectively. Also, d is inlet PVA concentration (mg/L). Each element within the process and disturbance transfer matrices were determined by fitting the experimental data to the structure of a first-order plus time delay (FOPTD) transfer function, elucidated below:

$$G_{ij}(s) = \frac{K_p}{1 + \tau s} e^{-\theta s} \quad (3)$$

Where, K_p is steady state gain, τ is time constant, and θ is the input-to-output time delay. Equation (4) represents the dynamic model for the process, incorporating the elements of transfer matrices derived from experimental data as detailed in our previous study (Hamad et al., 2021):

$$\begin{bmatrix} y_1 \\ y_2 \end{bmatrix} = \begin{bmatrix} \frac{0.4409e^{-0.715s}}{0.79s+1} & \frac{0.15909e^{-0.934s}}{2.098s+1} \\ \frac{0.4815s+1}{0.0719e^{-0.78s}} & \frac{1.207s+1}{0.0557e^{-0.5065s}} \end{bmatrix} \begin{bmatrix} u_1 \\ u_2 \end{bmatrix} + \begin{bmatrix} \frac{0.420e^{-0.875s}}{2.314s+1} \\ \frac{1.961s+1}{-0.006} \end{bmatrix} u_3 \quad (4)$$

The following section of the study delves into the importance of investigating potential interactions among the process parameters in a MIMO system prior to the controller design. It assesses the significance of these interactions and provides an overview of the approach to select the optimum MV/CV pairs effectively.

4. INTERACTIONS EVALUATION IN A MIMO SYSTEM

The block diagram representing the process defined by (4) is illustrated in Figure 2, where the interactive nature of the MIMO system is evident. However, this interaction needed to be quantified. An essential analytical tool for evaluating interactions among MVs and CVs within a MIMO system is

the relative gain array (RGA) computation. The RGA yields valuable insights not solely about identifying the existence or absence of interaction (also known as coupling) but also extends to assessing the magnitude and directionality of available interactions. Furthermore, it aids in the identification of optimal control pairs by determining the most effective MV for controlling a specific CV (Wang et al., 2018).

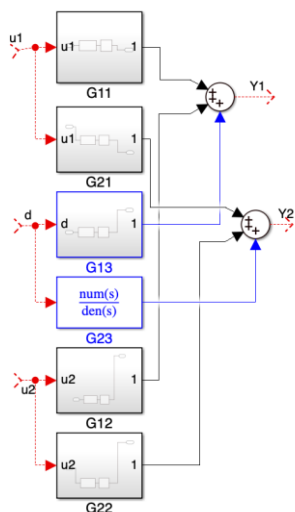


Figure 2. Block diagram of the coupled multi-input (u_1 and u_2), multi-output (y_1 and y_2) process, incorporating the influence of process disturbance (d), for degradation of PVA in a UV/H₂O₂ photoreactor.

The matrix RGA for a 2×2 MIMO system is calculated using the following equations:

$$\text{RGA} = \Lambda = \begin{bmatrix} \lambda_{11} & \lambda_{12} \\ \lambda_{21} & \lambda_{22} \end{bmatrix} = \begin{bmatrix} \lambda_{11} & 1 - \lambda_{11} \\ 1 - \lambda_{22} & \lambda_{22} \end{bmatrix} \quad (5)$$

Where, the parameter λ_{ij} signifies the association between the i^{th} CV and the j^{th} MV. In a 2×2 coupled system, as illustrated in Figure 3, the derivation of parameter λ_{11} is obtained from the following equations:

$$\lambda_{11} = \frac{\left(\frac{\Delta y_1}{\Delta u_1}\right)_{u_2=\text{constant}}}{\left(\frac{\Delta y_1}{\Delta u_1}\right)_{y_2=\text{constant}}} \quad (6)$$

The numerator in the equation signifies the dynamic response of y_1 to variations in u_1 , holding u_2 constant. Meanwhile, the denominator depicts the dynamic response of y_1 to changes in u_1 under the condition while y_2 is held constant at its setpoint. The alternative explanation is that each element in the RGA matrix signifies the proportion of the direct effect relative to the summation of both direct and indirect effects of an MV on a CV. Also, each element represents the ratio of the open-loop to closed-loop relationship between an MV and a CV. Utilizing the definition above for the λ_{ij} to substitute related transfer functions (TFs) into (6), followed by simplification, yields the subsequent equation for determining λ_{11} and λ_{22} in a 2×2 MIMO system:

$$\lambda_{11} = \lambda_{22} = \frac{1}{1 - \frac{K_{12}K_{21}}{K_{11}K_{22}}} \quad (7)$$

Where, K_{ij} represents the steady-state gain in the relationship between the i^{th} CV and the j^{th} MV.

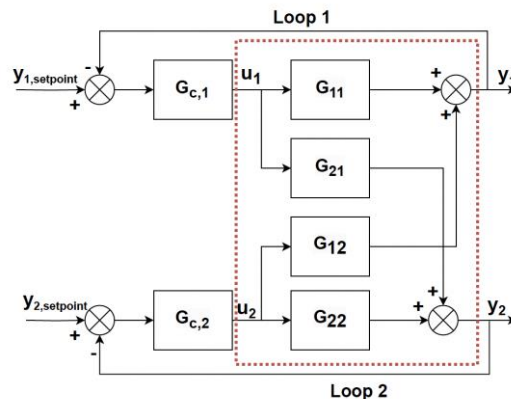


Figure 3. Block diagram of a 2×2 coupled MIMO.

In the RGA matrix, a λ_{ij} element of 0 denotes that the i^{th} CV remains unaffected by the j^{th} MV, while a value of 1 signifies complete reliance of the i^{th} CV on the j^{th} MV (non-interacting loops). Any deviations from the values of 0 or 1 in λ_{ij} indicate interactions or coupling between related MV and CV. The magnitude of these deviations serves as an indicator of the extent of interaction. If λ_{ij} is between 0 and 1, decoupling may not be necessary, and selecting appropriate pairs is viable. A positive λ_{ij} , within this range, signifies interaction between control loops, where MV_j affects not only CV_i, but other CVs. However, considering the RGA definition, as long as λ_{ij} is between 0 and 1, the indirect effect is generally weaker than the direct effect. In such cases, achieving effective control of CV_i by adjusting MV_j necessitates a higher controller gain than non-interactive control loops, potentially leading to instability as the gain approaches its ultimate values. In the worst-case scenario, λ_{ij} may fall outside the 0 to 1 range. In that case, considering a 2×2 MIMO system, as the summation of λ_{ij} in all rows and columns of the RGA equals 1, two λ_{ij} values exceed 1, and two are less than zero. The farther these values deviate from 0 and 1, the more challenging it becomes to control the system without decoupling measures. Effectively managing such systems may require the elimination of interactions through decoupling methods. Utilizing the RGA matrix also aids in selecting optimal pairs (optimal loops) of MV/CV. For non-interactive 2×2 MIMO systems, it is advised to choose pairs with a λ_{ij} value of 1, as a λ_{ij} of 0 implies no influence of the MV on the CV. In interactive systems, the preference is for pairs exhibiting positive λ_{ij} values, with a value as close to 1 as possible. Particularly in highly interactive systems, caution is warranted against choosing pairs with negative λ_{ij} values, as this decision can pose control challenges and induce instability in the closed-loop system. Negative λ_{ij} values signify a correlation between the i^{th} CV and j^{th} MV in the opposite direction, indicating that the impact of the MV_j on the other CV is more significant than its effect on CV_i and

occurs in a negative direction. Choosing such a pair with a negative λ_{ij} results in an oscillatory and unstable closed-loop. The following section elaborates on the necessity of decoupling highly interactive systems prior to the controller design.

5. DECOUPLING OF CONTROL LOOPS

Over time, PID controllers have maintained their prominence as the most extensively utilized controllers in industrial applications. This enduring popularity can be attributed to their straightforward implementation and operational simplicity, rendering them a favoured selection across diverse industrial sectors unless their performance is deemed inadequate (Garrido et al., 2016). The tuning of these controllers can be conducted manually without the requirement for sophisticated programming tools. Thus, the primary motivation of this study is to adopt a multi-loop control strategy utilizing PID-FB controllers instead of employing advanced and complicated controllers such as MPC.

In attaining the control goals within a multi-loop control framework for a highly interactive MIMO, decoupling becomes a prerequisite before controller design. Decoupling is an advanced control strategy that eliminates interaction among control loops, ensuring an MV exclusively influences the intended CV without affecting other CVs. The primary outcome of the decoupling process is maintaining stability in multi-loop control systems. A practical approach for decoupling involves the design of decouplers, which essentially are feedforward (FF) controllers. These decouplers treat an MV as a disturbance for other FB control loops to neutralize its impact on any FB loop except the targeted one. Such FF decouplers for a 2×2 MIMO system are illustrated in Figure 4 and are formulated as below:

$$D_{12} = -\frac{G_{12}}{G_{11}} \quad (8)$$

$$D_{21} = -\frac{G_{21}}{G_{22}} \quad (9)$$

Where, G_s are process TFs, as previously described and illustrated in Figure 4. By formulating the mathematical relationship between y_i and $y_{i,setpoint}$ for the control loops depicted in Figure 4, and subsequently substituting D values with (8) and (9), followed by simplifications, two decoupled control loops are obtained. The corresponding decoupled loops are illustrated in Figure 5. After deriving the decoupled loops, individual PID controllers can be tuned for each loop.

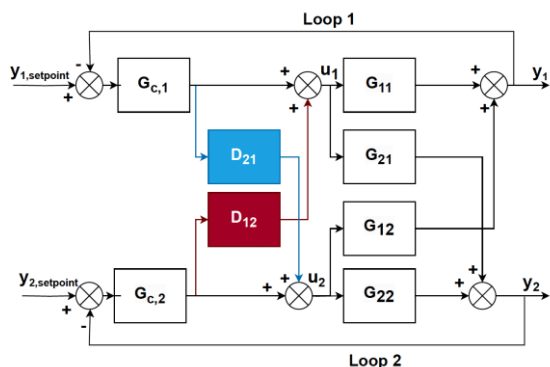


Figure 4. Block diagram of a 2×2 coupled MIMO including FF decouplers D_{12} and D_{21} .

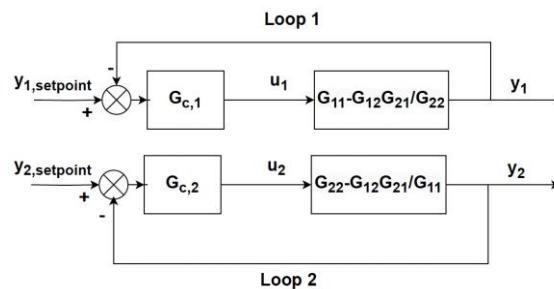


Figure 5. Block diagram of a 2×2 decoupled MIMO.

6. RESULTS AND DISCUSSION

Using the theoretical knowledge in Section 4 and the dynamic model of the 2×2 MIMO system in this study, as outlined in (4), the matrix of steady-state gains is presented below:

$$K = \begin{bmatrix} K_{11} & K_{12} \\ K_{21} & K_{22} \end{bmatrix} = \begin{bmatrix} 0.4409 & 0.15909 \\ 0.0719 & 0.0557 \end{bmatrix} \quad (10)$$

Subsequently, employing (5) and (7), the RGA matrix for the system is as follows:

$$\Lambda = \begin{bmatrix} 1.8719 & -0.8719 \\ -0.8719 & 1.8719 \end{bmatrix} \quad (11)$$

The computed RGA reveals interactions among the process parameters due to λ_{ij} values outside the 0 to 1 range. The positive value of $\lambda_{11} = \lambda_{22} = 1.8719$ indicates the necessity for controlling effluent TOC (y_1) and residual H_2O_2 (y_2) by manipulating PVA feed flowrate (u_1) and inlet H_2O_2 concentration (u_2), respectively. However, owing to the high interaction, evident in the deviation of λ_{ij} from 0 to 1 range, the need for decoupling persists. Additionally, the goal is to avoid observing changes in any CV except for the targeted one by adjusting a specific MV. Consequently, following the methodology outlined in Section 5, two decouplers, as presented below, were designed for this study:

$$D_{12} = -\frac{G_{12}}{G_{11}} = \frac{0.0766s+0.15909}{0.5322s+0.4409} e^{-0.219s} \quad (12)$$

$$D_{21} = -\frac{G_{21}}{G_{22}} = \frac{0.1508s+0.0719}{0.044s+0.0557} e^{-0.2735s} \quad (13)$$

Subsequently, the decoupled loops for the process are shown in Figure 6. Figure 6 aligns with the simplified decoupled system in Figure 5, with the only distinction being the inclusion of a disturbance in the process. The PID controllers in decoupled FB loops shown in Figure 6 were tuned using the embedded PID tuner in MATLAB Simulink. The resulting parameters and performance for the PID-FB controllers, which emphasize their fast rise time, settling time, small overshoot, and stable response, are summarized in Tables 1 and 2. In this study, the control objective was setpoint tracking and disturbance rejection. In order to evaluate the performance of the designed control strategy in setpoint tracking, in one simulation experiment, arbitrary step changes to both CVs setpoints were applied. These included effluent TOC setpoint changing from 560 to 450 mg/L at $t = 100$ s and residual H_2O_2 setpoint changing from 34 to 25 mg/L at $t = 50$ s. Step changes to setpoints were introduced at various simulation times to demonstrate that, as a result of decoupling, alterations in the

setpoint of a CV and the subsequent adjustments in the corresponding MV do not impact the other CV. All simulations to investigate the system response were conducted in MATLAB Simulink.

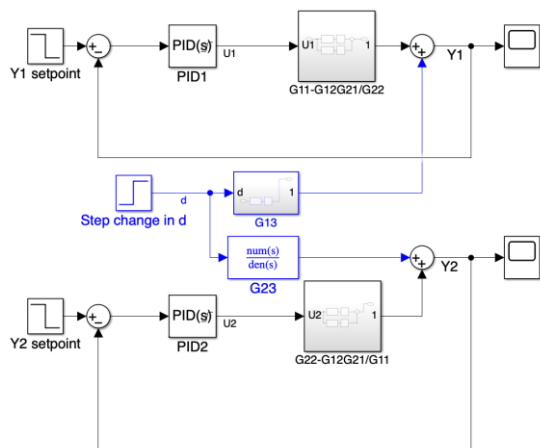


Figure 6. Closed-loop block diagram of the decoupled MIMO for degradation of PVA in UV/H₂O₂ photoreactors.

Table 1. Tuned parameters of PID controllers.

Controller	P	I	D	N
PID-FB 1	1.882	2.575	-2.8973	0.6062
PID-FB 2	49.4601	31.0615	-34.4535	1.028

Table 2. Performance analysis for the PID controllers.

Controller	t_r (s)	t_s (s)	Overshoot%	Closed-loop stability
PID-FB 1	1.06	6.17	2.58	Stable
PID-FB 2	1.25	7.78	5.73	Stable

Note: t_r : Rise Time, t_s : Settling Time.

The response of the decoupled closed-loop system to setpoint changes was simulated for 720 seconds, aligning with the average residence time of the process. However, to maintain clarity in the graphs, only the first 130 seconds of results are depicted due to the rapid settling time. Figures 7 and 8 illustrate that the proposed multi-loop control strategy effectively regulates the process to track setpoint trajectories with minimal overshoot and offsets. It is evident from Figures 7 and 8 that changing the setpoint of one CV does not disrupt the other CV. For instance, altering the setpoint of residual H₂O₂ at 50 seconds has no impact on effluent TOC at 50 seconds and beyond, as illustrated in Figure 7.

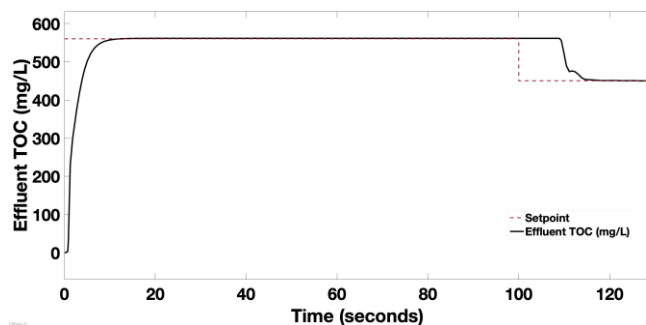


Figure 7. Decoupled system response: effluent TOC (mg/L) to setpoint trajectories, during 200 s simulation.

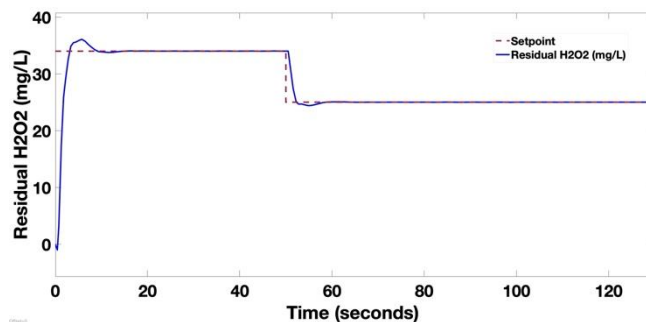


Figure 8. Decoupled system response: residual H₂O₂ (mg/L) to setpoint trajectories, during 200s simulation.

In another simulation, the performance of the control system in disturbance rejection was evaluated. While keeping setpoints constant at their corresponding optimum values, a disturbance was induced by a step change in the inlet PVA concentration from 1000 to 1500 mg/L at $t=100$ s, depicted in Figure 9-a. Due to the rapid settling time, the system response only for the first 130 seconds is presented. Figures 9-b to 9-c demonstrate the ability of the system to swiftly regulate itself (within less than 20 seconds) after a significant disturbance. Results in a fast return of CVs to their designated setpoints. Additionally, it was observed that the alteration in the inlet PVA concentration had a more significant effect on effluent TOC than residual H₂O₂, as it directly introduces additional TOC content into the process influent.

The final phase assessed the realizability of the designed decouplers for real-world application. A decoupler is deemed realizable if it functions as a lag compensator, not a lead one. Considering (12) and (13), the negative sign in the exponential term indicates lag compensators. In conclusion, the designed decouplers are realizable.

7. CONCLUSIONS

In this study, the interaction among process variables in a 2×2 MIMO system, representing PVA degradation in UV/H₂O₂ photoreactors, was identified by RGA analysis. RGA also revealed well-paired MV/CV sets. Later, decoupling was performed by adding FF decouplers in the closed-loop structure of the MIMO to address the interaction of the system. Then, PID controllers in decoupled loops were tuned, and their performances in setpoint trajectories and disturbance rejection were evaluated through simulation in MATLAB Simulink.

Results demonstrated the effectiveness of the proposed control strategy in both setpoint tracking and disturbance rejection with a high rise and settling time and negligible overshoot. Lastly, realizability analysis confirmed the practical applicability of the decouplers.

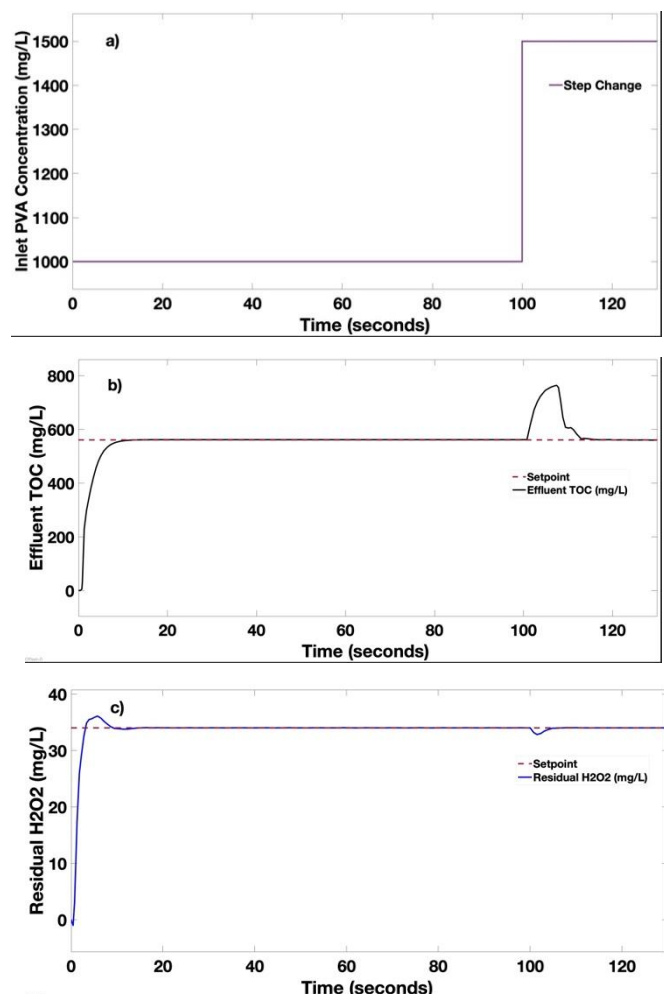


Figure 9. a) Applied 50% step change in the inlet PVA concentration (mg/L), b) response of effluent TOC (mg/L), and c) response of residual H₂O₂ (mg/L) to the applied step change in the decoupled system, during 130 s simulation.

Despite the demonstrated effectiveness of the proposed control method, it is crucial to acknowledge the complexity of real-world operating conditions. Various disturbances, including fluctuations in influent pH, temperature, and feed flow rates, can impact system performance. These disturbances may occur simultaneously or follow patterns other than a step change. Therefore, depending on the specific operating environment, assumptions made in this study may vary, necessitating a re-evaluation of the controllers performance for operating in more complex conditions.

8. ACKNOWLEDGEMENTS

The financial support of the Natural Sciences and Engineering Research Council of Canada (NSERC) and the Toronto Metropolitan University Faculty of Engineering and Architectural Science Dean's Research Fund is greatly appreciated.

9. REFERENCES

- Astrom, K. J., Johansson, K. H., and Wang, Q.-G. (2001). Design of decoupled PID controllers for MIMO systems, *Proceeding of American Control Conference*. <https://doi.org/10.1109/ACC.2001.946038>
- Garrido, J., Vázquez, F., and Morilla, F. (2016). Multivariable PID control by decoupling. *International Journal of Systems Science*, 47(5), 1054–1072. <https://doi.org/10.1080/00207721.2014.911390>
- Hamad, D. (2015). Experimental Investigation of Polyvinyl Alcohol Degradation in UV/H₂O₂ Photochemical Reactors Using Different Hydrogen Peroxide Feeding Strategies [Doctor of Philosophy Thesis]. Ryerson University, Toronto, Canada.
- Hamad, D., Mehrvar, M., and Dhib, R. (2018). Photochemical Kinetic Modeling of Degradation of Aqueous Polyvinyl Alcohol in a UV/H₂O₂ Photoreactor. *Journal of Polymers and the Environment*, 26(8), 3283–3293. <https://doi.org/10.1007/s10924-018-1190-y>
- Hamad, D., Dhib, R., and Mehrvar, M. (2021). Identification and Model Predictive Control (MPC) of Aqueous Polyvinyl Alcohol Degradation in UV/H₂O₂ Photochemical Reactors. *Journal of Polymers and the Environment*, 29(8), 2572–2584. <https://doi.org/10.1007/s10924-020-02031-z>
- Lin, Y. P., Dhib, R., and Mehrvar, M. (2021). Recent advances in dynamic modeling and process control of PVA degradation by biological and advanced oxidation processes: A review on trends and advances. *Environments*, 8(11). <https://doi.org/10.3390/environments8110116>
- Parsa, Z., Dhib, R., and Mehrvar, M. (2022). Modelling and Optimization Study on Biodegradability Enhancement of PVA-Contained Wastewater in a Continuous UV/H₂O₂ photoreactor. *Proceedings of the 6th International Conference of Recent Trends in Environmental Science and Engineering (RTESE'22)*. <https://doi.org/10.11159/rtese22.231>
- Parsa, Z., Dhib, R., and Mehrvar, M. (2024). Dynamic Modelling, Process Control, and Monitoring of Selected Biological and Advanced Oxidation Processes for Wastewater Treatment: A Review of Recent Developments. *Bioengineering*, 11(2), 189. <https://doi.org/10.3390/bioengineering11020189>
- Parsa, Z., Mehrvar, M., and Dhib, R. (2023). Biodegradability Improvement of Water-Soluble-Polymers in Wastewater in a Continuous UV/H₂O₂ Photoreactor. *Proceedings of the 7th International Conference of Recent Trends in Environmental Science and Engineering (RTESE 2023)*. <https://doi.org/10.11159/rtese23.116>
- Wang, B., Quingchuan, Z., Shuang, K., and Ji, K. (2018). Coupling Analysis of AC Motors Based on Relative Gain Array. *Proceeding of IEEE 3rd Advanced Information Technology, Electronic and Automation Control Conference*. <https://doi.org/10.1109/IAEAC.2018.8577826>